Hindawi
Advances in Civil Engineering
Volume 2019, Article ID 6735623, 16 pages
https://doi.org/10.1155/2019/6735623

Research Article

Displacement Solution of Salt Cavern with Shear Dilatation Behavior Based on Hoek-Brown Strength Criterion

Huabin Zhang, Qingqing Zhang, and Laigui Wang

Mechanical and Engineering College of Liaoning Technical University, Fuxin 123000, China

Correspondence should be addressed to Huabin Zhang; lgd_zhb@163.com

Received 1 January 2019; Revised 3 March 2019; Accepted 10 March 2019; Published 4 April 2019

Academic Editor: Giovanni Garcea

In this study, an analytical solution of stress, strain, and displacement, in the elastic and plastic zone is proposed. The solution is derived on the basis of ideal elastoplastic mechanical model of spherical salt cavern with shear dilatation behavior, by adopting Hoek-Brown (H-B) criterion. The solution obtains not only in small and large strain stage but also in creep stage. The proposed solution is validated, by comparison of the obtained results with numerical results in FLAC3D. The results indicate that the result obtained adopting the H-B criterion is closer to that one obtained adopting the Mohr-Coulomb (M-C). The H-B criterion is more applicable for the salt cavern construction as it considers the structural characteristics of the rock salt formation. The displacement difference obtained by two different methods decreases with the increase of GSI or running pressure, but it increases with the enlarged angle of dilation. The influence of different assumptions of elastic strain of plastic zone on displacements is more significant under large strain conditions. The influence of the angle of dilation on displacements is more obvious when the elastic strain of plastic zone is given to stationary values, and the influence degree increases with the enlarged angle of dilation. Under the same conditions, the creep displacement decreases with the increase of GSI, and both the creep displacement and the effect degree enhance with the enlarged dilation angle. The proposed solutions can be used in the stability analysis of surrounding rock in the construction and operation of salt cavern storage.

1. Introduction

A study on the analytical solution to stress and deformation of surrounding rock of simplified mechanical model is carried out based on the stress and strain redistribution. The redistribution is caused by the salt cavern storage formation in underground caverns, which is formed in the salt cavern building with water solution in the deep salt formations. And the rock mass strength at the cavity wall is reduced during salt cavern leaching. In order to obtain reasonable deformation of surrounding rock, many scholars have carried out the analysis of stress and strain of surrounding rock based on the simplified mathematical model of underground caverns. Park and Kim [1] proposed a closed-form solution for the displacement of the plastic zone of a circular tunnel, by using the nonassociated flow rules combined with three definition methods for elastic strains of plastic zone. Sun et al. [2] proposed an approximate analytical solution for the circular tunnel with joints and analyzed the influence relationship of the rock mass parameters based on the H-B strength criterion and the assumption of the stress field under axisymmetrical and asymmetric stress conditions. Jimenez et al. [3] proposed a new equivalent method for symmetric circular tunnel based on the H-B criterion by assuming that the stress field in the plastic zone is linear. Fraldi and Guarracino [4] predicted the possibility of collapse accidents in circular tunnel excavation and proposed a simple and accurate solution based on the H-B, and they proposed elastoplastic analytical solutions of ground rock of tunnel based on convergence-confinement method. Rojat et al. [5] established a new dimensionless form of the generalized H-B failure criterion, completed the convergence calculations for tunnel in-depth by

considering the problem of edge effects, and proposed new exact formulations for the case of an associated H-B plastic potential. Wang et al. [6] determined the H-B criterion parameters of the anhydrite intact rock and rock mass and performed a numerical simulation in FLAC3D. In order to analyze the stability of the deep cavern group, they proposed the element safety factor method based on the generalized H-B and stress distribution. Lu et al. [7] studied the plane strain elastic-plastic problem for the circular tunnel in H-B media subjected to nonhydrostatic stress, proposed the analytical optimization method for nonlinear equations. A solution of the elastoplastic interface is presented for the plane strain problem of a pressurized circular tunnel in H-B media subjected to nonhydrostatic stress at infinity. Llamas et al. [8] proposed a mini-CAES concept where the cavity is shallower than current CAES, applying the H-B criterion for the calculation of the subsidence profile. Other scholars have conducted a lot of research on the plane problem of circular tunnel [9–12]. Hou et al. [13] proposed semianalytical and seminumerical solutions of the axisymmetric circular tunnel under ideal elastoplastic conditions by adopting the Levy–Mises constitutive relation and generalized H-B failure criterion. Cai et al. [14] analyzed the elastoplastic solution of the circular chamber under uniform stress field by the dimensionless H-B criterion and proposed that displacement can be effectively controlled by improving rock mass quality for soft rock chamber. Zhang et al. [15], by taking comprehensive influences of intermediate principal stress, brittle softening, dilation characteristic, Young's modulus, and elastic strains in the plastic zone into account, established a new solution for the displacement and characteristic curve of the plastic zone of the surrounding rock. Moreover, Liu et al. [16] analyzed the salt rock deformation under triaxial compressive stress condition, indicated the large compressive deformation properties of salt rock under higher confining pressure, and analyzed the stress-strain characteristics of the salt rock by using the logarithmic strain. Using large deformation (logarithmic strain), the problem of cavity expansion has been analyzed [17–20] in consideration of the shear dilation and the strain softening. The long-term behavior of salt causes the convergence of the salt cavity, so it is necessary to consider the stability and shrinkage of the cavity of long-term operation. Zhang and Xiong [21] proposed an analytical solution for the displacement of elasto-visco-plastic ground around the circular tunnel, which can not only reflect the effects of dilatancy and plastic softening on displacements but also take account into the creep property of the ground. Sun [22] discussed the research on rock rheology and the engineering applications. Yuan et al. [23] carried out viscoelastic-plasticity analysis of the rheological problem of deep soft rock tunnel taking the Drucker-Prager strength criterion as the plastic yielding conditions, and expanding effect of plastic zone is considered. Hou et al. [24] proposed an iterative algorithm based on the creep solution of constant passive support force for axisymmetric round well and used the iterative algorithm to calculate the creep deformation of surrounding rock. Wen et al. [25] and Cao et al. [26] determined an analytical solution for the rheological deformation of the surrounding rock by the generalized H-B criterion combined with the Nishihara model and considered the influence of the volumetric dilatancy on the solution. The theoretical solutions for the deep spherical salt cavern are related to the complicated mathematical deduction; however, there is only a few theoretical research studies on the deep spherical cavern, especially the analytical solution of the rheological and the large deformation of the surrounding rock in the salt cavern storage project, and M-C and Drucker-Prager criterion has been used. Because the H-B criterion introduced the influence on rock mass underground construction, which can reflect the disturbance effect on salt cavern leaching process, it is more suitable for the practical engineering. From this point of view, this paper studied the elastoplastic (including two forms, i.e., logarithmic strain and engineering strain) and viscoelastic-plastic displacement of surrounding rock in the salt cavern storage by introducing the H-B criterion combined with the equilibrium equation. This study is expected to provide theoretical reference for the design and construction of underground salt cavern.

2. Simplified Model for Salt Spherical Cavern Storage

In this study, the salt cavern storage is simplified into a deep spherical cavern. The distribution of the far field stress tends to be a approximate homogeneous hydrostatic pressure field where the stress value is p_0. The rock mass of the surrounding rock is homogeneous and isotropic. The radius of the salt cavern is designed as R_0, and the running pressure p_i homogeneously acts on the cavern wall. Gravity and side pressure coefficient are not considered in this study. The coordinate origin of the salt cavern mechanics model is set in the center of the spherical cavern to meet the spherical symmetry. Initial in situ stress and running pressure are considered in this study; the salt rock conforms to the hypothesis of the ideal elastoplastic model, and the compressive stresses are considered positive. During the cavern building and operating process, there exist the elastic and plastic zones in the surrounding rock of the salt cavity. The region away from the salt cavern ($R_p \longrightarrow \infty$) is in an elastic state, while the near-zone of the cavern ($R_0 \longrightarrow R_p$) enters into a plastic state. R_p is designed as plastic radius. Figure 1 is the elastoplastic analysis model for surrounding rock of spherical salt cavern adits. And the surrounding rock satisfies continuity conditions in the elastic-plastic interface.

3. Strength Criterion

The generalized H-B criterion which is widely used can be written as

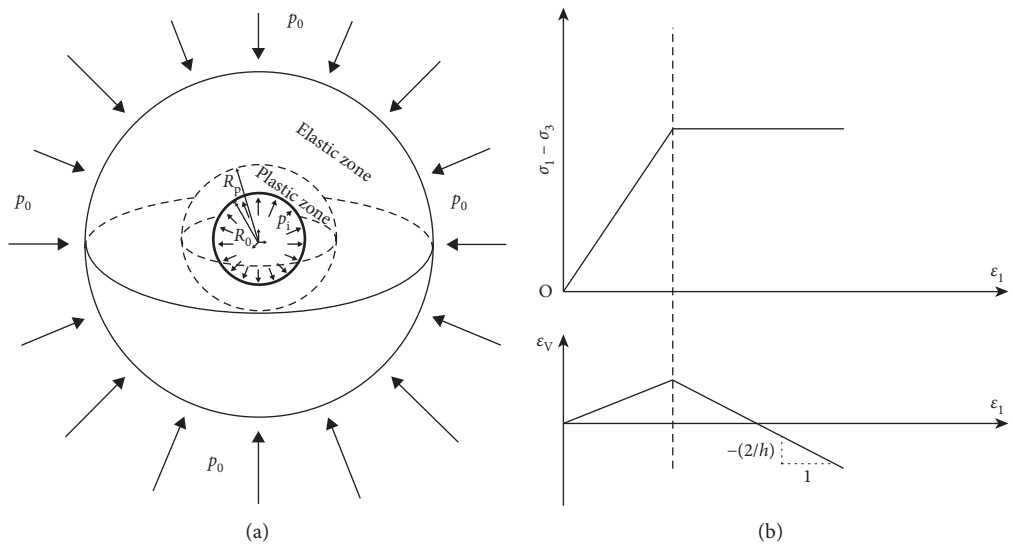

Figure 1: The ideal elastoplastic model of spherical salt cavern. (a) The elastic-plastic model for spherical salt cavern. (b) Material behavior model of salt rock.

$$\sigma_1 = \sigma_3 + \sigma_{ci}\left(m_b\frac{\sigma_3}{\sigma_{ci}} + s\right)^a, \tag{1}$$

where σ_{ci} is the uniaxial compressive strength of the intact rock (MPa) and m_b, s, and a are the petrographic constants of the rock mass.

The disturbance coefficient D of the rock mass is introduced into the H-B criterion and a new method for parameter (m_b, s, and a) value selection is proposed [27]. The parameters are based on the geological strength index (GSI). m_b, s, and a are given as

$$\begin{cases} m_b = m_i e^{(\mathrm{GSI}-100/28-14D)}, \\ s = e^{\mathrm{GSI}-100/9-3D}, \\ a = \dfrac{1}{2} + \dfrac{1}{6}\left(e^{-\mathrm{GSI}/15} - e^{-20/3}\right), \end{cases} \tag{2}$$

where GSI is the geological strength index, which varies from 10 to 100, it will be taken as 10 for a poor rock mass. D is the disturbance coefficient of the rock mass, which varies from 0 for an undisturbed in situ rock mass to 1 for a very disturbed rock mass. m_i is the petrographic parameter reflecting the degree of stiffness of rock mass, which varies from 0 to 25 for the rock mass. s and a are petrographic parameters of the rock mass, which varies from 0 to 1, and the parameter $a = 1/2$ for most intact rock.

4. Elastoplastic Analytical Solutions

4.1. Stress, Strain, and Displacement in Elastic Zone. Because of the symmetry of the underground cavity, in spherical coordinate system, the corresponding relationships between principal stress and the spherical coordinate stress are $\sigma_1 = \sigma_2 = \sigma_\theta = \sigma_\varphi$, $\sigma_3 = \sigma_r$, and there are same corresponding relationships for strains. Hence, the differential equation of equilibrium can be expressed as

$$\frac{d\sigma_r}{dr} + \frac{2}{r}(\sigma_r - \sigma_\theta) = 0. \tag{3}$$

In the elastic zone, where $R_p \longrightarrow \infty$, the boundary condition can be written as $\sigma|_{r=R_p} = \sigma_{R_p}$. Based on Lame's formula, compressive stresses are reckoned to be positive, and the stress in the elastic zone can be expressed as

$$\begin{cases} \sigma_r^e = \left(1 - \left(\dfrac{R_p}{r}\right)^3\right)p_0 + \left(\dfrac{R_p}{r}\right)^3 \sigma_{R_p}, \\ \sigma_\theta^e = \left(1 + \dfrac{1}{2}\left(\dfrac{R_p}{r}\right)^3\right)p_0 - \dfrac{1}{2}\left(\dfrac{R_p}{r}\right)^3 \sigma_{R_p}. \end{cases} \tag{4}$$

Based on the elasticity and without considering the effect of the initial in situ stress p_0, strains can be written as

$$\begin{cases} \varepsilon_r = \dfrac{du}{dr} = \dfrac{1}{E}\left[(\sigma_r - p_0) - 2\mu(\sigma_\theta - p_0)\right], \\ \varepsilon_\theta = \dfrac{u}{r} = \dfrac{1}{E}\left[(\sigma_\theta - p_0) - \mu(\sigma_r + \sigma_\theta - 2p_0)\right]. \end{cases} \tag{5}$$

In the elastic region, at elastic-plastic interface, $r = R_p$, and the elastic strains can be expressed as

$$\begin{cases} \varepsilon_r^e = \dfrac{1}{2G}\left(\sigma_{R_p} - p_0\right), \\ \varepsilon_\theta^e = -\dfrac{1}{4G}\left(\sigma_{R_p} - p_0\right), \end{cases} \tag{6}$$

where $G = (E/(2(1+\mu)))$.

The displacement caused by the salt cavern building with water solution can be obtained as

$$u^{e}(r) = \frac{1}{4G}\left(\sigma_{R_p} - p_0\right)\frac{R_p^3}{r^2}. \tag{7}$$

4.2. Stress in Plastic Zone and Plastic Radius. The range of the plastic zone of salt cavern is $R_0 \le r \le R_p$, after combining equation (4) and considering the boundary condition $\sigma_r = \sigma_{R_p}$ at $r = R_p$. We can obtain that

$$\sigma_r^e\big|_{r=R_p} + 2\sigma_\theta^e\big|_{r=R_p} = 3p_0. \tag{8}$$

By substituting the radial and tangential stresses in plastic zone with $r = R_p$ into equation (1), the nonlinear H-B strength criterion can be expressed as

$$\sigma_\theta^p = \sigma_r^p + \sigma_{ci}\left(\frac{m_b}{\sigma_{ci}}\sigma_r^p + s\right)^a. \tag{9}$$

After combining equations (3) and (9) and considering the boundary condition $\sigma_r^p = p_i$ at $r = R_0$, we can obtain the radial stress in the plastic zone:

$$\sigma_r^p = \frac{\sigma_{ci}}{m_b}\left\{\left[2(1-a)m_b\ln\left(\frac{r}{R_0}\right) + \left(m_b\frac{p_i}{\sigma_{ci}} + s\right)^{(1-a)}\right]^{(1/(1-a))} - s\right\}. \tag{10}$$

Combining equation (8) and considering the stress is continuous at the interface, $r = R_p$, we can obtain that

$$\sigma_r^p + 2\sigma_\theta^p = 3p_0. \tag{11}$$

Combining equations (9) and (11) and considering the boundary condition $\sigma_r^p\big|_{r=R_p} = \sigma_{R_p}$, we can obtain that

$$2\sigma_{ci}\left(\frac{m_b}{\sigma_{ci}}\sigma_{R_p} + s\right)^a + 3\sigma_{R_p} - 3p_0 = 0. \tag{12}$$

Combining nonlinear equation (12) and using iteration method, the radial stress in the plastic zone can be determined. And, the tangential stress can be obtained based on equation (9). Then, with equation (10), the plastic radius R_p is

$$R_p = R_0 e^{\left(\left((m_b/\sigma_{ci})\sigma_{R_p}+s\right)^{1-a} - \left((m_b(p_i/\sigma_{ci})+s)\right)^{1-a}/2(1-a)m_b\right)}. \tag{13}$$

As $R_p \ge R_0$, the stress at the elastic-plastic interface should satisfy $\sigma_{R_p} \ge p_i$. And we inferred that the plastic radius is related to the in situ stress p_0, the running pressure p_i, and the H-B criterion parameters σ_{ci}, m_i, s, and a.

4.3. Deformation Analysis in Plastic Zone. When the surrounding rock of salt cavern enters into plastic state, in order to determine the displacement in the plastic zone, it is necessary to establish displacement differential equations for surrounding rock using the geometric equation. Therefore, it is necessary to determine the relationship between the strain components of the plastic zone where the total strain consists of elastic and plastic strain.

$$\begin{cases} \varepsilon_r = \varepsilon_r^e + \varepsilon_r^p, \\ \varepsilon_\theta = \varepsilon_\theta^e + \varepsilon_\theta^p. \end{cases} \tag{14}$$

Many scholars have put forward different definitions for the elastic strain in the plastic zone. Some consider the elastic strain is very small, and it does not change. Hence, the elastic strain in the plastic zone is equal to the elastic strain at the elastic-plastic interface in the elastic zone. Others consider the stress-strain relationship conforms to the thick-walled cylinder theory and the generalized Hooke's law. The elastic strain in the plastic zone is a variable which changes with the position of the surrounding rock [15]. In this study, the elastic strain in the plastic zone is discussed under the above two cases.

At the same time, the relationship between the plastic strain components is established using the flow rule. Based on the nonassociated flow law, plastic strain increments can be written as

$$\frac{d\varepsilon_r^p}{d\varepsilon_\theta^p} = -\frac{2}{h}, \tag{15}$$

where $h = (1 - \sin\psi)/1 + \sin\psi$ and ψ is the angle of dilation, which is obtained by triaxial compressive test.

After combining equations (14) and (15), we can obtain that

$$hd\varepsilon_r + 2d\varepsilon_\theta = hd\varepsilon_r^e + 2d\varepsilon_\theta^e. \tag{16}$$

Assuming the elastic strain in the plastic zone is a constant value, which is equal to the elastic strain at $r = R_p$ in the elastic zone and after combining equations (6) and (16), we can obtain that

$$h\varepsilon_r + 2\varepsilon_\theta = h\varepsilon_r^e + 2\varepsilon_\theta^e = f_1(r), \tag{17}$$

where $f_1(r) = (h-1)\delta$, $\delta = (1/2G)(\sigma_{R_p} - p_0)$.

Assuming the elastic strain in the plastic zone is a variable and abiding by Hooke's law, after combining equations (5) and (16), we can obtain that

$$h\varepsilon_r + 2\varepsilon_\theta = h\varepsilon_r^e + 2\varepsilon_\theta^e = f_2(r), \tag{18}$$

where $f_2(r) = (1/2G(1+\mu))\{(h-2\mu)\sigma_r + 2(1-\mu-h\mu)\sigma_\theta - (h+2)(1-2\mu)p_0\}$.

To simplify the problem, we make the H-B parameter $a = 0.5$. Equation (10) can be written as

$$\sigma_r^p = p_i + 2A_1\ln\left(\frac{r}{R_0}\right) + A_2\ln^2\left(\frac{r}{R_0}\right), \tag{19}$$

where $A_1 = \sqrt{m_b\sigma_{ci}p_i + s\sigma_{ci}^2}$, $A_2 = m_b\sigma_{ci}$. After combining equations (9) and (19), the tangential stress can be written as

$$\sigma_\theta^p = \sigma_r^p + A_1 + A_2\ln\left(\frac{r}{R_0}\right). \tag{20}$$

By substituting equations (19) and (20) into the function $f_2(r)$, we can obtain that

$$f_2(r) = \frac{1}{2G(1+\mu)}\left\{B_1 + B_2\ln\left(\frac{r}{R_0}\right) + B_3\ln^2\left(\frac{r}{R_0}\right)\right\}, \tag{21}$$

where $B_1 = (h+2)(1-2\mu)(p_i - p_0) + 2(1-\mu-h\mu)A_1$, $B_2 = 2(h+2)(1-2\mu)A_1 + 2(1-\mu-h\mu)A_2$, $B_3 = (h+2)(1-2\mu)A_2$.

In the infinitesimal deformation case, relationships of strains and displacement are as follows:

$$\varepsilon_r = \frac{du}{dr}, \qquad \varepsilon_\theta = \varepsilon_\varphi = \frac{u}{r}. \tag{22}$$

By substituting equation (22) into equation (17), differential equation for the radial displacement $u(r)$ can be written as $h(du/dr) + 2(u/r) = f_1(r)$. The total displacement in the plastic zone can be obtained as

$$u_c^p(r) = e^{-(2/h)\int(1/r)dr}\left[C_1 + \int \frac{f_1(r)}{h} e^{(2/h)\int(1/r)dr} dr\right] = C_1 r^{-(2/h)} + \frac{(h-1)\delta}{2+h} r. \tag{23}$$

Then, considering continuous condition at the elastic-plastic interface, we can obtain that $C_1 = (1/2)(4 - h/2 + h)\delta R_p^{(2/h)+1}$.

The displacement $u_c^p(r)$ in equation (23) is caused by building, and it is obtained without considering the variation of the elastic strain in plastic zone.

In the same way, by substituting equation (22) into equation (18), differential equation for the radial displacement $u(r)$ can be written as $h(du/dr) + 2(u/r) = f_2(r)$. The total displacement in the plastic zone is

$$u_v^p(r) = e^{-(2/h)\int(1/r)dr}\left[C_2 + \int \frac{f_2(r)}{h} e^{(2/h)\int(1/r)dr} dr\right] = C_2 r^{-(2/h)} + \frac{1}{2G(1+\mu)} \frac{r^{-(2/h)}}{h} \int \left[B_1 + B_2 \ln\left(\frac{r}{R_0}\right) + B_3 \ln^2\left(\frac{r}{R_0}\right)\right] r^{(2/h)} dr,$$

$$u_v^p(r) = C_2 r^{-(2/h)} + \frac{r}{2G(1+\mu)(2+h)} \cdot \left[B_1 + B_2\left(\ln\left(\frac{r}{R_0}\right) - \frac{1}{(2/h)+1}\right) + B_3\left(\ln^2\left(\frac{r}{R_0}\right) - \frac{2}{(2/h)+1}\ln\left(\frac{r}{R_0}\right) + \frac{2}{((2/h)+1)^2}\right)\right]. \tag{24}$$

Then, considering continuous condition at the elastic-plastic interface, we can obtain that

$$C_2 = \left\{\frac{1}{2}\delta - \frac{1}{2G(1+\mu)(2+h)} \cdot \left[B_1 + B_2\left(\ln\left(\frac{R_p}{R_0}\right) - \frac{1}{(2/h)+1}\right) + B_3\left(\ln^2\left(\frac{R_p}{R_0}\right) - \frac{2}{(2/h)}\ln\left(\frac{R_p}{R_0}\right) + \frac{2}{((2/h)+1)^2}\right)\right]\right\} R_p^{(2/h)+1}. \tag{25}$$

The displacement $u_v^p(r)$ in equation (24), which is caused by building, is obtained with assuming the elastic strain in the plastic zone abiding by Hooke's law.

Table 1 shows displacements, which are obtained based on perfect elastoplastic constructive model, using H-B criterion and considering different definitions for elastic strain in the plastic zone.

In the case of $\psi = 0^\circ$ (no plastic volume change), the displacements in the plastic zone are discussed.

(a) Assuming that the elastic strain in the plastic zone is a constant value, then $f_1(r) = 0$, $C_1 = (1/2)\delta R_p^3$; the displacement in the plastic zone is

$$u_c^p(r) = \frac{1}{2}\delta \frac{R_p^3}{r^2}, \tag{26}$$

which is the same with that in the elastic zone, i.e., equation (7).

(b) Assuming the elastic strain in the plastic zone is a variable, which abides by Hooke's law, we can obtain that

$$f_2(r) = \frac{1-2\mu}{2G(1+\mu)}\left\{3(p_i - p_0) + 2A_1 + 2(3A_1 + A_2)\ln\left(\frac{r}{R_0}\right) + 3A_1 \ln^2\left(\frac{r}{R_0}\right)\right\},$$

$$C_2 = \left\{\frac{1}{2}\delta + \frac{1}{6G(1+\mu)}\left[B_1 + B_2\left(\ln\left(\frac{R_p}{R_0}\right) - \frac{1}{3}\right) + B_3\left(\ln^2\left(\frac{R_p}{R_0}\right) - \frac{2}{3}\ln\left(\frac{R_p}{R_0}\right) + \frac{2}{9}\right)\right]\right\} R_p^{(2/h)+1}. \tag{27}$$

The displacement in the plastic zone is

Table 1: Summary of the displacements in the plastic zone.

Geometric equations	$\varepsilon_r = (du/dr)\,\varepsilon_\theta = (u/r)$
Displacement in the plastic zone in a compact form	$r^{-(2/h)}\left\{C_i + (1/h)\int f_i(r) r^{(2/h)} dr\right\}, \quad i = 1, 2$
$i = 1$	The elastic strain in the plastic zone is a constant value, which equals to the elastic strain at the elastic-plastic interface $r = R_0$ in the elastic zone
$i = 2$	The elastic strain in the plastic zone is a variable, which abides by Hooke's law
$f_1(r)$	$(h-1)\delta$
$f_2(r)$	$(1/2G(1+\mu))\left\{B_1 + B_2\ln(r/R_0) + B_3\ln^2(r/R_0)\right\}$
C_1	$(1/2)((4-h)/(2+h))\delta R_p^{(2/h)+1}$
C_2	$\{(1/2)\delta - (1/2G(1+\mu)(2+h))[B_1 + B_2(\ln(R_p/R_0) - 1/(2/h)+1) + B_3(\ln^2(R_p/R_0) - 2/(2/h)+1)\ln(R_p/R_0) + 2/((2/h)+1)^2]\}R_p^{(2/h)+1}$

$$u_v^p(r) = \frac{1}{2}\delta\frac{R_p^3}{r^2} + \frac{1}{6G(1+\mu)} \cdot \left\{\left[B_1 + B_2\left(\ln\left(\frac{r}{R_0}\right) - \frac{1}{3}\right) + B_3\left(\ln^2\left(\frac{r}{R_0}\right) - \frac{2}{3}\ln\left(\frac{r}{R_0}\right) + \frac{2}{9}\right)\right]r - \left[B_1 + B_2\left(\ln\left(\frac{R_p}{R_0}\right) - \frac{1}{3}\right) + B_3\left(\ln^2\left(\frac{R_p}{R_0}\right) - \frac{2}{3}\ln\left(\frac{R_p}{R_0}\right) + \frac{2}{9}\right)\right]\frac{R_p^3}{r^2}\right\}. \tag{28}$$

5. Large Strain Solutions

According to the finite deformation theory, it is considered that the strain in the plastic zone is distributed in a logarithmic form. The logarithmic strain (true strain) can reflect the sum of the relative strain increments at various stages of total deformation, and it is closer to the actual accumulation process of deformation and the degree of large deformation. This study introduced the logarithmic strain $\varepsilon = \int_{r_0}^{r} dl/l = \ln(r/r_0)$ to represent large deformation of salt cavern [16, 17]. The logarithmic strain indicates that the initial position r_0 gradually changes to r which will undergo several intermediate states during the deformation process of the plastic zone; the variables r and r_0 cannot be treated as constants during the calculation. Then, the displacement of the salt cavern in plastic zone is derived adopting the large strain.

For large strain problem, the geometric equation can be written as

$$\varepsilon_r = \ln\frac{dr}{dr_0}, \qquad \varepsilon_\theta = \varepsilon_\varphi = \ln\frac{r}{r_0}. \tag{29}$$

Combing equations (17) and (29), we can obtain that

$$h\ln\frac{dr}{dr_0} + 2\ln\frac{r}{r_0} = f_1(r), \qquad \ln\left(\frac{r}{r_0}\right)^{(2/h)}\frac{dr}{dr_0} = \frac{f_1(r)}{h}, \tag{30}$$

where $r_0 \in [r_o, R_p - u_{R_p}]$, $r \in [r, R_p]$, and u_{R_p} denotes the displacement in the elastic zone at elastic-plastic interface. The integration of equation (30) leads to the following expression for the displacement.

$$u_{ls,c}^p(r) = r - r_0 = r - \left\{\left(R_p - u_{R_p}\right)^{((h+2)/h)} - e^{-((h-1)\delta/h)}\left(R_p^{((h+2)/h)} - r^{((h+2)/h)}\right)\right\}^{h/(h+2)}. \tag{31}$$

For the case of large deformation in plastic zone, which is caused by cavern building, equation (31) can fully express the displacement, which is obtained without consideration of the variation of elastic strain in the plastic zone.

In the same way, combing equations (18) and (39), we can obtain that

$$h\ln\frac{dr}{dr_0} + 2\ln\frac{r}{r_0} = f_2(r). \tag{32}$$

The integration of equation (32) leads to the following form for displacement

$$u_{\mathrm{ls,v}}^{\mathrm{p}}(r) = r - r_0 = r - \left\{\left(R_{\mathrm{p}} - u_{R_{\mathrm{p}}}\right)^{((h+2)/h)} - \frac{h+2}{h}\int_r^{R_{\mathrm{p}}} e^{-\left(f_2(r)/h\right)} r^{(2/h)}\, dr\right\}^{h/(h+2)}. \tag{33}$$

For the case of large deformation in plastic zone, which is caused by cavern building, equation (33) can fully express the displacement, which is obtained assuming the elastic strain and the total stress in the plastic zone abiding by Hooke's law. By the method of element changing in integral, equation (33) can be written as

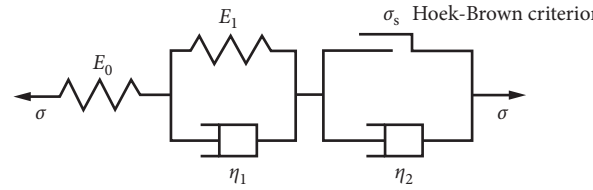

Figure 2: Nishihara model.

$$u_{\mathrm{ls,v}}^{\mathrm{p}}(r) = r - r_0 = r - \left\{\left(R_{\mathrm{p}} - u_{R_{\mathrm{p}}}\right)^{((h+2)/h)} - \frac{h+2}{h}\int_0^1 e^{-(1/2G(1+\mu))\left(\left\{B_1+B_2\ln\left(\left(\left(R_{\mathrm{p}}-r\right)x+r\right)/R_0\right)+B_3\ln^2\left(\left(\left(R_{\mathrm{p}}-r\right)x+r\right)/R_0\right)\right\}/h\right)}\left(\left(R_{\mathrm{p}}-r\right)x+r\right)^{2/h}\left(R_{\mathrm{p}}-r\right)dx\right\}^{h/(h+2)}. \tag{34}$$

Then, the numerical solution of equation (34) can be obtained by Romberg integration.

When $\psi = 0^{\circ}$ (no plastic volume change), assuming the elastic strain in the plastic zone is a constant value, the displacement in the plastic zone can be obtained:

$$u_{\mathrm{ls,c}}^{\mathrm{p}}(r) = r - r_0 = r - \left\{\left(R_{\mathrm{p}} - u_{R_{\mathrm{p}}}\right)^3 - \left(R_{\mathrm{p}}^3 - r^3\right)\right\}^{1/3}. \tag{35}$$

Assuming the elastic strain in the plastic zone is a variable, the displacement in the plastic zone can be written as

$$u_{\mathrm{ls,v}}^{\mathrm{p}}(r) = r - r_0 = r - \left\{\left(R_{\mathrm{p}} - u_{R_{\mathrm{p}}}\right)^3 - 3\int_r^{R_{\mathrm{p}}} e^{-(1/2G(1+\mu))\left\{B_1+B_2\ln\left(r/R_0\right)+B_3\ln^2\left(r/R_0\right)\right\}} r^2\, dr\right\}^{1/3}. \tag{36}$$

6. Viscoelastic-Plastic Deformation Analysis

The period of salt cavern building is long, and the working state is periodically injecting or producing circulated process. Creep displacement will take place in the surrounding rock in elastic and plastic zones, when the salt cavern kept operation at a reasonable inner pressure. It is necessary to investigate creep displacements, without considering the creep failure. As shown in Figure 2, the classical Nishihara model, which can fully reflect elasticity, viscoelasticity, and viscoplasticity in the transient creep and steady creep process [20, 21, 28], can be used to analyze the creep deformation of the surrounding rock of salt cavern.

The 1D creep constitutive equations for the classical Nishihara model are

$$\begin{cases} \varepsilon = \dfrac{\sigma}{E_0} + \dfrac{\sigma}{E_1}\left(1 - e^{-\left(E_1/\eta_1\right)t}\right), & \sigma < \sigma_{\mathrm{s}}, \\ \varepsilon = \dfrac{\sigma}{E_0} + \dfrac{\sigma}{E_1}\left(1 - e^{-\left(E_1/\eta_1\right)t}\right) + \dfrac{\sigma - \sigma_{\mathrm{s}}}{\eta_2}t, & \sigma \geq \sigma_{\mathrm{s}}, \end{cases} \tag{37}$$

where E_0 stands for the elastic modulus, E_1 denotes the viscoelastic modulus, and η_1 and η_2 are the viscosity coefficients. The 1D creep constitutive equations show that the creep strain is related to time and the differential stress.

6.1. Viscoelastic Deformation Analysis. The Nishihara model degenerates to a three-parameter model when the stress of the surrounding rock of salt cavern is lower than the yield stress σ_{s}; operators of the Nishihara model are listed in Table 2.

Table 2: The Nishihara model's operators.

Viscoelastic model's operators	Laplace space forms
$\overline{P}'(s)$	$1 + (\eta_1/(G_0 + G_1)s)$
$\overline{Q}'(s)$	$(G_0G_1/G_0 + G_1) + (\eta_1 G_0/G_0 + G_1)s$
$(\sigma_{R_p} - p_0)$	$(\overline{\sigma}_{R_p} - \overline{p}_0)/s$

Taking Laplace inverse transform on equation (37), the creep strain in viscoelastic zone can be written as

$$\begin{cases} \varepsilon_r^c = -\dfrac{\sigma_\theta - \sigma_r}{2G_1}\left(1 - e^{-(G_1/\eta_1)t}\right), \\ \varepsilon_\theta^c = \dfrac{\sigma_\theta - \sigma_r}{2G_1}\left(1 - e^{-(G_1/\eta_1)t}\right). \end{cases} \tag{38}$$

The analytic equation of displacement, i.e., equation (7) can be directly converted to Laplace space form as

$$\overline{u}^e(r) = \frac{\overline{P}'(s)}{4\overline{Q}'(s)}\left(\sigma_{R_p} - p_0\right)\frac{R_p^3}{r^2}. \tag{39}$$

Substituting the Nishihara model's operators, which are presented in Table 2, into equation (39) and then taking Laplace inverse transform on equation (39), we can obtain the viscoelastic displacement in the viscoelastic zone $R_p \longrightarrow \infty$, which is caused by caverns building, as the following expression:

$$u_c^e(t,r) = \frac{1}{4}\left[\frac{1}{G_0} + \frac{1}{G_1}\left(1 - e^{-(G_1/\eta_1)t}\right)\right]\left(\sigma_{R_p} - p_0\right)\frac{R_p^3}{r^2}, \tag{40}$$

where $G_0 = E/2(1+\mu)$, G_1 is viscoelastic shear modulus which can be determined experimentally, and η_1 is viscoelastic shear coefficient which can be determined experimentally.

6.2. Viscoplastic Deformation Analysis. It is complicated to solve the displacement of surrounding rock of salt cavern in plastic zone $R_0 \le r \le R_p$. The total strain of the surrounding rock is $\varepsilon = \varepsilon^e + \varepsilon^p + \varepsilon^c$, which includes elastic strain ε^e, plastic strain ε^p, and creep strain ε^c.

In order to determine the total strain of plastic zone, assuming neither the elastic strain nor the creep strain causes the volume change, we can obtain that

$$\begin{cases} \varepsilon_r^e + 2\varepsilon_\theta^e = 0, \\ \varepsilon_r^c + 2\varepsilon_\theta^c = 0. \end{cases} \tag{41}$$

Based on equation (15), the strain increments relationship can be written as

$$\begin{aligned} h\varepsilon_r + 2\varepsilon_\theta &= h\varepsilon_r^e + 2\varepsilon_\theta^e + h\varepsilon_r^c + 2\varepsilon_\theta^c \\ &= 2(1-h)I_0, \end{aligned} \tag{42}$$

where $I_0 = \varepsilon_\theta^e + \varepsilon_\theta^c$.

In order to simplify the problem, assuming the elastic strain in the viscoplastic zone is continuous at the viscoelastic-viscoplastic interface, based on equation (6), the tangential elastic strain in the viscoplastic zone ε_θ^e can be obtained. Hence, the elastic strain ε_θ^e in the viscoplastic zone is a constant independent of both the time t and the distance away from the center.

The creep strain in the viscoplastic zone is obtained using viscoelasticity analysis method. When $\sigma \ge \sigma_s$, the 3D creep strain in the plastic zone can be written as

$$\begin{cases} \varepsilon_r^c = -\dfrac{\sigma_\theta - \sigma_r}{2G_1}\left(1 - e^{-(G_1/\eta_1)t}\right) - \dfrac{\sigma_\theta - \sigma_r - \sigma_s}{2\eta_2}t, \\ \varepsilon_\theta^c = \dfrac{\sigma_\theta - \sigma_r}{2G_1}\left(1 - e^{-(G_1/\eta_1)t}\right) + \dfrac{\sigma_\theta - \sigma_r - \sigma_s}{2\eta_2}t. \end{cases} \tag{43}$$

The yield stress is defined as the difference between the tangential stress and the radial stress at elastic-plastic interface. Combining equations (19) and (20), we can obtain that $\sigma_s = A_1 + A_2\ln(R_p/R_0)$. Combining equations (4) and (38) and combining equations (19), (20), and (43), creep strains $\varepsilon_{\theta p}^c\big|_{r=R_p}$ and $\varepsilon_{\theta p}^c\big|_{r=R_0}$ can be obtained, respectively.

$$\begin{cases} \varepsilon_{\theta p}^c\big|_{r=R_p} = -\dfrac{3}{4G_1}\left(1 - e^{-(G_1/\eta_1)t}\right)\left(\sigma_{R_p} - p_0\right), \\ \varepsilon_{\theta p}^c\big|_{r=R_0} = \dfrac{A_1}{2G_1}\left(1 - e^{-(G_1/\eta_1)t}\right) + \left(\dfrac{A_2\ln\left(R_p/R_0\right)}{2\eta_2}\right)t. \end{cases} \tag{44}$$

Assuming that the creep strain in the viscoplastic zone, which can be approximated by the average of the creep strain in the viscoplastic zone at the elastoplastic interface and the creep strain at the cavern wall calculated based on the differential stress, is an r-independent value [23, 26] and substituting ε_θ^e and equations (36) into (34), we can obtain that $I_0 = \varepsilon_\theta^e + (1/2)(\varepsilon_{\theta p}^c\big|_{r=R_p} + \varepsilon_{\theta p}^c\big|_{r=R_0})$.

The parameter I_0 depends only on the time t and does not depend on the position of the surrounding rock r. Referring to the solving approach in the above chapter and combing equations (22) and (42), the first-order nonhomogeneous constant coefficient differential equation for $u(r)$ can be written as $h(du/dr) + 2(u/r) = 2(1-h)I_0$. The viscoplastic displacement in the plastic zone can be obtained as

$$u_c^p(t,r) = J_0 r^{-(2/h)} + \frac{2(1-h)}{2+h}I_0 r, \tag{45}$$

where $J_0 = \{1/4[(1/G_0) + (1/G_1)(1 - e^{-(G_1/\eta_1)t})](\sigma_{R_p} - p_0) - (2(1-h)/2 + h)I_0\}R_p^{(2/h)+1}$.

When $t = 0$, equation (45) is the same as equation (23), which can describe the displacement in the plastic zone without consideration of the creep strain.

When $\psi = 0^\circ$ (no plastic volume change), the equation (45) is the same as equation (40), which can describe the displacement in the viscoelastic zone, and we can obtain that

$$u_c^p(t,r) = \frac{1}{4}\left[\frac{1}{G_0} + \frac{1}{G_1}\left(1 - e^{-(G_1/\eta_1)t}\right)\right]\left(\sigma_{R_p} - p_0\right)\frac{R_p^3}{r^2}. \quad (46)$$

7. Case Study and Discussion

Taking the salt cavern gas storage being excavated in China as an example, the structural parameters and mechanical parameters are given in Table 3.

Table 4 Shows the mechanical parameters of salt rock which are involved in the model.

The literature investigation results show that GSI and m_i of the H-B criterion have a similar significant influence on the stress and displacement of the surrounding rock. By taking the different values 60 and 80 of GSI into account, a study has been conducted to evaluate their influences on the displacement. Table 5 shows the other parameters for calculation. In order to validate the result in this paper, as shown in Figure 3, the displacements, which are obtained adopting two different definitions of elastic strain of the plastic zone, and stresses are contrasted; it is not surprising that the results agree with previous outcomes [29].

In order to validate the analytical solutions, numerical computations are carried out for the salt cavity storage. Under the same conditions, the displacement of the surrounding rock can be derived based on the H-B and M-C criterions with the aid of the FLAC3D. In order to establish the model of the salt cavern under uniform stress field, set stress boundary conditions in FLAC3D 5.0. As shown in Figure 4, principal stress and displacement, which are obtained under the same conditions, are extracted from FLAC3D by setting GSI = 60 and using the H-B criterion in FLAC3D. Figure 5 shows the comparison between numerical solutions and analytical solutions. In Figure 5, the results show that the distribution of the principal stress and the displacement is fundamentally identical with the analytical solution. The results indicate that displacements in the plastic zone gradually decrease with the distance away from the salt cavity; the difference of the displacements that obtained under different conditions gradually declined. But the difference between displacements on the plastic zone still remains under different conditions. Compared with numerical solutions at the cavity wall, the analytical one is smaller. No matter the analytical solutions or the numerical solutions, the displacement for M-C rock mass lies in the range of results when GSI = 80 to GSI = 60. The results close to that based on the M-C criterion can be obtained by appropriate readjustment of the H-B criterion parameter GSI, but the H-B criterion, which introduced the structural characteristics of the rock mass, has better applicability than the M-C criterion.

7.1. Effect of Large Strain and Small Strain: Theory to Results. The displacement in the plastic zone is plotted in Figure 6 for cases of H-B parameter GSI = 60 and GSI = 80. It can be seen from Figure 6 that the range of the plastic zone reduced (the plastic radius decreased from 44.79 m to 35.91 m) and the displacement has decreased, with the H-B parameter GSI increasing from 60 to 80. The difference of the displacement, which caused no matter by two different strain theories or by two different elastic strain definitions, is greater, when GSI = 60. When the elastic strain of plastic zone takes on stationary values, the displacement obtained with small strain theory is larger than large strain theory. But when the elastic strain abides by Hooke's law, the displacement obtained with small strain theory is smaller than large strain theory. In large strain stage, for cases of GSI = 60 and GSI = 80, the difference of displacement at the cavity wall that is caused by two definitions for elastic strains, is 0.030 m and 0.008 m, respectively. However, in small strain stage, for cases of GSI = 60 and GSI = 80, the difference of displacement is 0.008 m and 0.003 m, respectively. It indicates that the difference of displacements has a little difference for good rock mass; while it has great difference for poor rock mass, such as broken rock mass, fractured rock mass, or rock formation with natural fractures. In large strain stage, for two cases of different assumptions about the elastic strains, the difference of displacement at the cavity wall, which is caused by two different values of GSI, is 0.035 m and 0.057 m, respectively. In small strain stage, the difference of displacements for different assumptions about the elastic strains is 0.044 m and 0.039 m, respectively. It indicates that the influence of different hypothesis of the elastic strains on the displacement is more obvious, as considering large strain.

Figure 7 shows the displacements, which are obtained by taking two different elastic strain definitions in the plastic zone and two different strain theories into account, in the plastic zone for cases of $\psi = 0$, $\psi = 0.25\varphi$, and $\psi = 0.5\varphi$. It can be seen from Figure 7 that the displacement at the same point increases with the enlarged dilation angle. The displacements intersect with each other at one point (displacement at elastoplastic interface) with the distance away from the salt cavity, which indicate that the influence of dilation angle on the displacements gradually reduces. When $\psi = 0$ (no plastic volume change), for cases of different elastic strain definitions, the displacements with reference to small strain are almost the same. It is important to note that when the displacement is obtained

Table 3: Parameters for salt cavern storage.

Radius of the salt cavern storage R_0	30 m
Far field pressure p_0	40 MPa
Running pressure of the salt cavern p_i	10 MPa
Elastic modulus of salt rock E	10 GPa
Poison ratio of salt rock μ	0.3
Dilation angel of salt rock ψ	0.25φ

Table 4: Parameters of salt rock.

Geological strength index GSI	σ_{ci} (MPa)	m_i	D	m_b	a	s	φ (°)	c (MPa)
60	24.4	4.1	0.2	0.84	0.5	0.0085	34.8	6.38
80	24.4	4.1	0.2	1.85	0.5	0.0925	34.8	6.38

Table 5: Dataset.

GSI		60			80	
R_p		44.787			35.906	
σ_{R_p}		24.889			19.558	
δ		−0.002			−0.003	
A1		14.479			22.526	
A2		20.456			45.237	
ψ	0	0.25ϕ	0.5ϕ	0	0.25ϕ	0.5ϕ
B1	−24.417	−21.700	−19.656	−17.979	−14.629	−12.108
B2	51.116	51.205	51.274	90.252	91.450	92.351
B3	24.547	23.473	22.664	54.285	51.909	50.121
C1	−89.836	−309.470	−1016.600	−62.492	−201.360	−619.664
C2	−89.836	−283.517	−871.787	−62.492	−184.473	−531.379

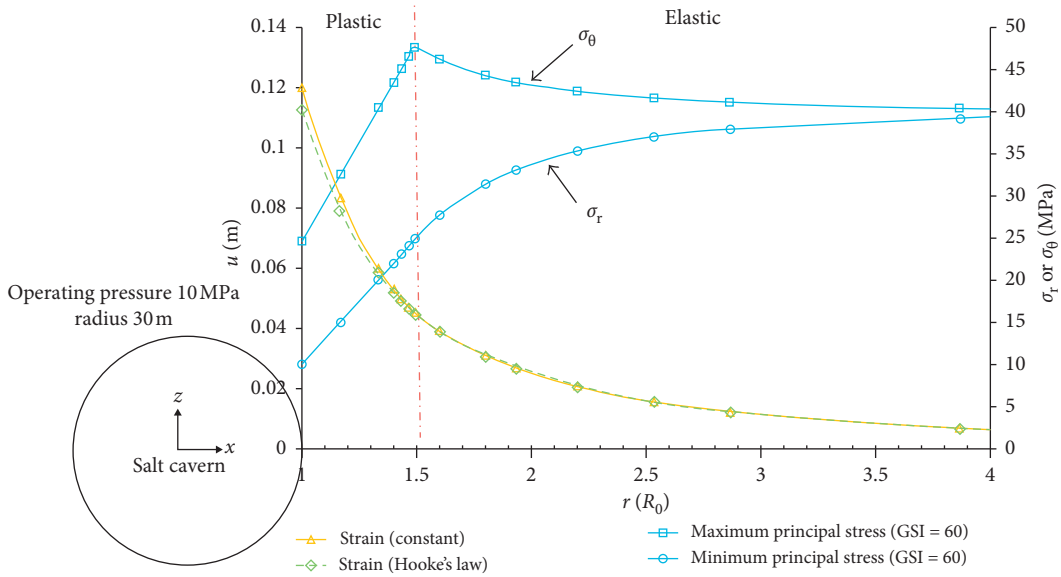

Figure 3: Displacements, stresses, and the plastic radius of the salt cavern (GSI = 60).

based on large strain theory, the various definitions of elastic strain in the plastic zone affect the displacements differently. Note that when the elastic strain takes a constant value, the displacements with reference to large deformation theory agree with the displacements with reference to small deformation theory; however, when the elastic strain conforms to Hooke's law, the displacement which is obtained based on large deformation theory is greater than the displacement obtained based on small deformation theory. When $\psi \neq 0$ (plastic volume increase), whether $\psi = 0.25\varphi$ or $\psi = 0.5\varphi$, the displacements obtained based on large strain are smaller than that one obtained based on small strain when the elastic strain of plastic zone is constant. However, the displacements obtained based on large strain are greater than those obtained based on small strain when the elastic strain abides by Hooke's law. The above results relate to the solutions obtained by using the semianalytical method of Romberg numerical integration. Figure 8 shows relationships between the dilation angles and the relative increment of the displacements at the cavity wall. It can be seen from Figure 8 that the relative increment increases linearly with the dilation angle. The dilation angle has the most significant influence on the displacement with reference to small strain, while it has the least influence on the displacement with reference to large strain when the elastic strain of plastic zone is constant.

Figure 9 illustrates relationships between the operation pressure and the displacement at the cavity wall. It can be seen from Figure 9, the displacement decreases with the increase of the operating pressure, and the maximum difference of the displacement is at operation pressure 2 MPa. The displacements at the cavity wall for different cases are 0.36 m, 0.39 m, 0.42 m, 0.55 m, and 0.74 m, respectively. There is difference between displacements obtained based on different strain theories. When the elastic strain in the plastic zone is constant, the displacement with reference to large strain theory is smaller than the one with reference to small strain theory. However, there is a contrary relationship between the displacements, which is closer to the numerical results, when the elastic strain conforms to Hooke's law. Therefore, appropriate control of inner pressure can reduce the displacements at the cavity wall effectively, and it can also reduce the impact of the two different elastic strain definitions and the two different strain theories.

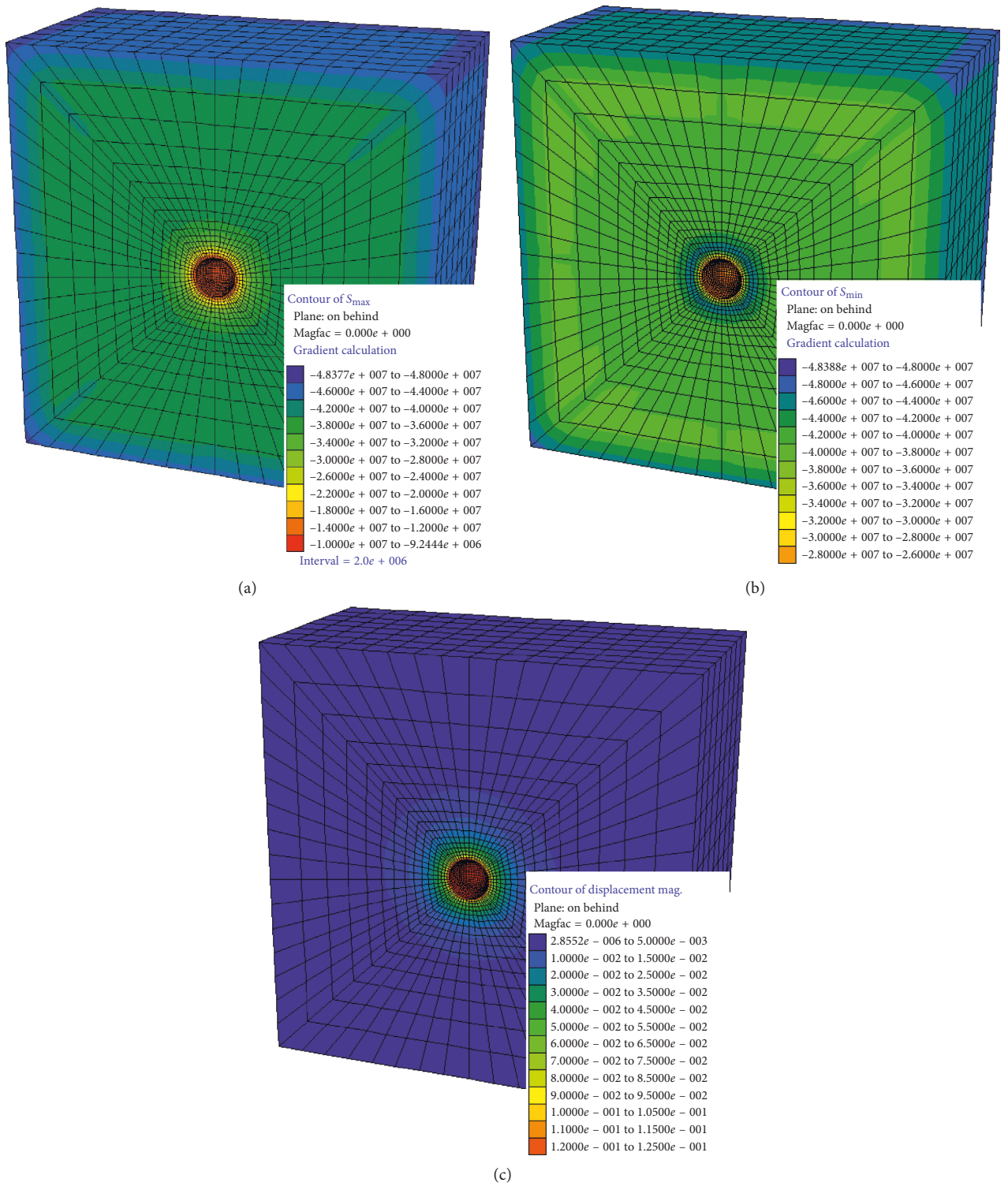

Figure 4: Principal stress and displacement (tensile stresses are considered positive, GSI = 60).

7.2. Results considering Rheological Properties. The creep curves of surrounding rock of the salt cavern have been obtained at $r = 30$ m and $r = 35$ m, by taking different values of GSI and taking the creep model parameters of surrounding rock of the salt cavern as shown in Table 6.

Take the point $r = 30$ m and $r = 35$ m as the observation points; it can be seen from Figure 10 that the rheological displacement equation derived in this result is correct. The displacements of the surrounding rock decrease with the increase of GSI; the higher the parameter GSI, the lower the displacement. The rheological displacement of the surrounding

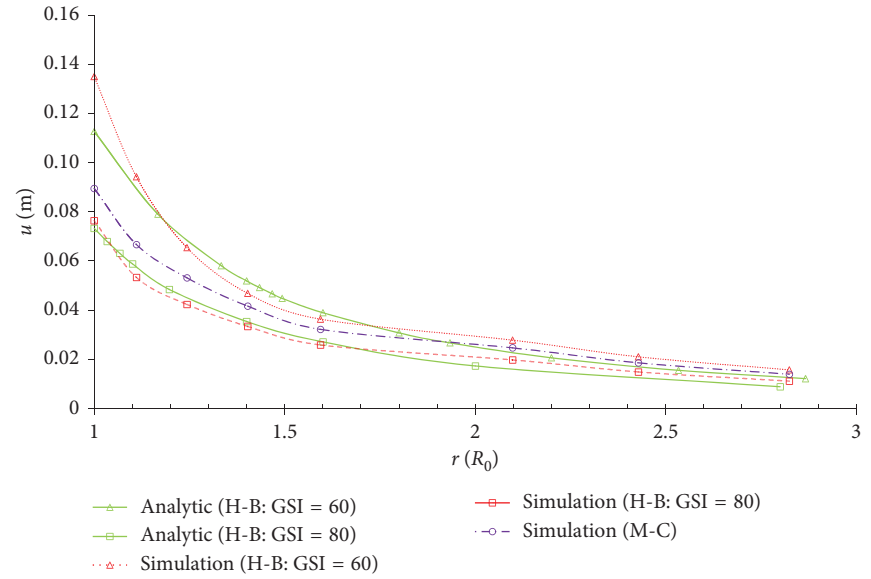

Figure 5: Comparison of displacements between analytical solution and numerical simulation results.

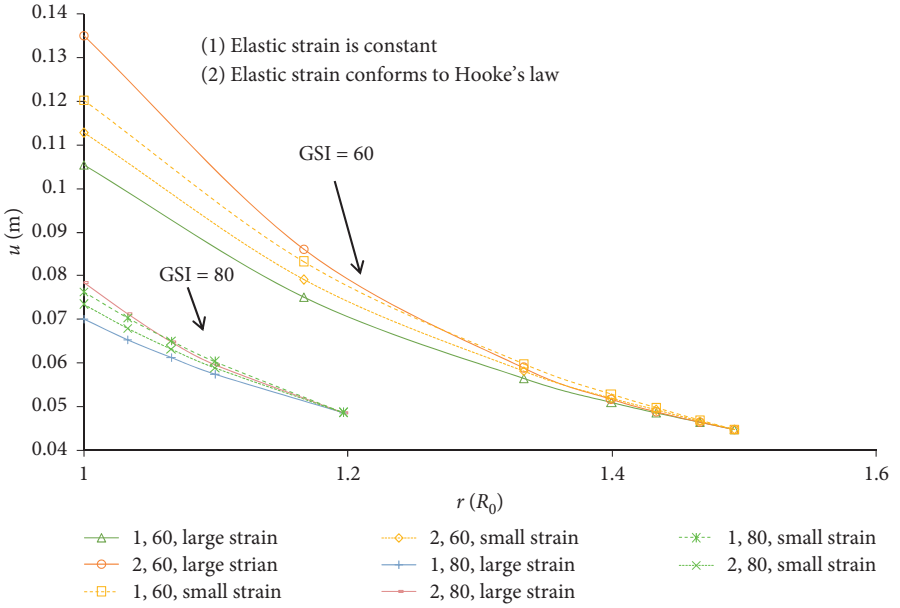

Figure 6: Relationships between plastic zone displacements and GSI (different elastic strain definitions and different strain theories).

rock can be well controlled and can enter the second creep stage (steady-state creep stage) faster. The displacements at the cavern wall still increase linearly in the second creep stage, and the increasing rate is related to the viscosity coefficient μ_2.

Figure 11 shows the relationship between time and creep displacements at the cavern wall for cases of $\psi = 0$, $\psi = 0.25\varphi$, and $\psi = 0.5\varphi$. As can be seen from Figure 11, the initial value of the creep displacement gradually decreases with the reduced angle of dilation at the cavern wall. The total creep displacement increased with the enlarged dilation angle within 200h. The dilation angle increases from 0 to 0.5φ, the creep displacements are 0.1 m, 0.13 m, and 0.16 m, respectively, and the relative values of displacement $(u(t = 200) - u(t = 0)/u(t = 0)) \times 100\%$ are 1.3%, 9.9%, and 16.2%, respectively. Both the variation gradient of the creep displacement rate and the creep rate in the steady-state creep stage increase with the enlarged dilation angle. Also, the region of the primary creep stage becomes larger with the enlarged dilation angle. Hence, the angle of dilation has great influence on the creep displacement.

8. Conclusions

(1) The results based on the spherical model and the simplified plane model for the salt cavern are different because of the difference of the balance

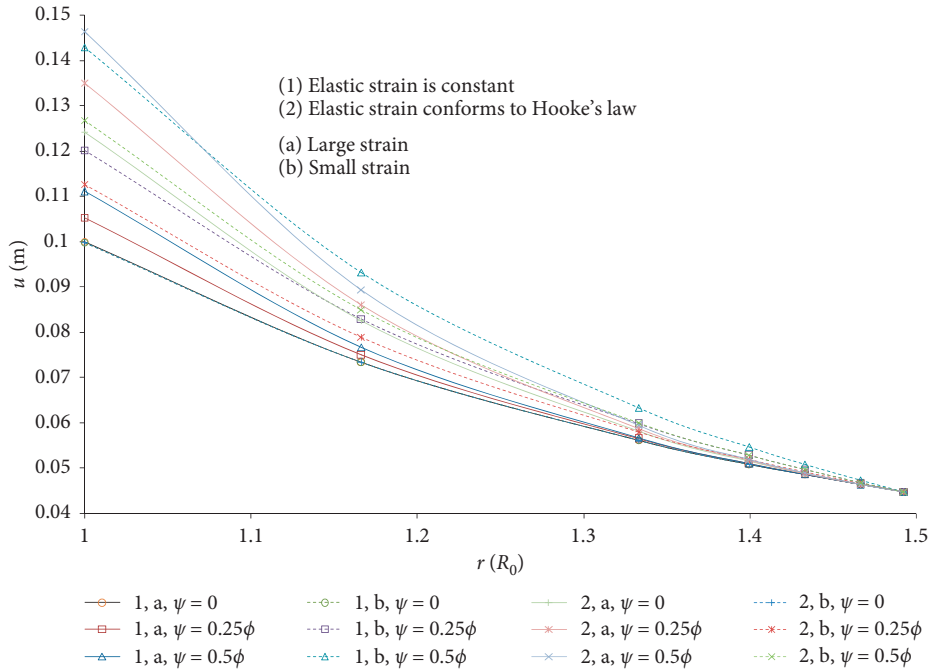

Figure 7: Relationships between plastic zone displacements and dilation angle (different elastic strain definitions and different strain theories).

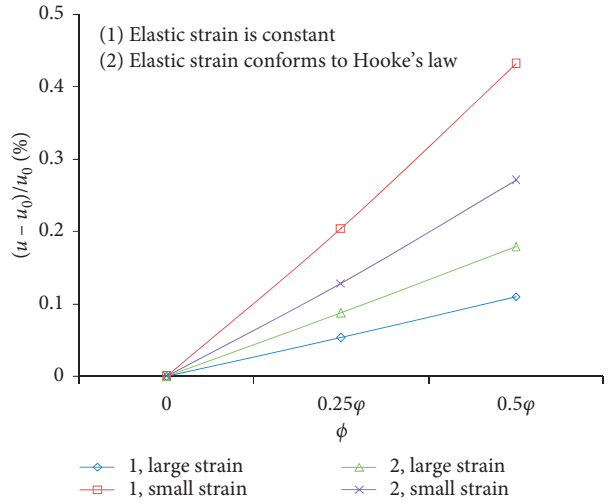

Figure 8: Relationships between displacements at the cavity wall and dilation angle (different elastic strain definitions and different strain theories).

equations, although the constitutive relation and the plastic flow rule are consistent in solving process. The results of the spherical model are more applicable to the natural conditions of the salt cavern storage.

(2) The displacements of plastic zone are analyzed by taking two different elastic strain definitions of plastic zone, large strain, and small strain into account. The influence of H-B parameter GSI, operating pressure, and dilation angle on the four analytical solutions is studied. The maximum difference of the displacements in the plastic zone is at the cavern wall. The difference decreased gradually with the distance away from the cavern wall. The displacements of the surrounding rock can be controlled effectively with the increase of the H-B parameter GSI or the operating pressure, while it increases with the enlarged dilation angle. When the elastic strain of plastic zone is constant, the displacements obtained based on large strain are smaller than that obtained based on small strain under the same conditions, while there is a contrary relationship when the elastic strain conforms to Hooke's law. The influence of different elastic strain definitions on the displacements that obtained based on large strain is more significant. When the elastic strain of plastic zone is constant, the influence of dilation angle on the displacements is most obvious,

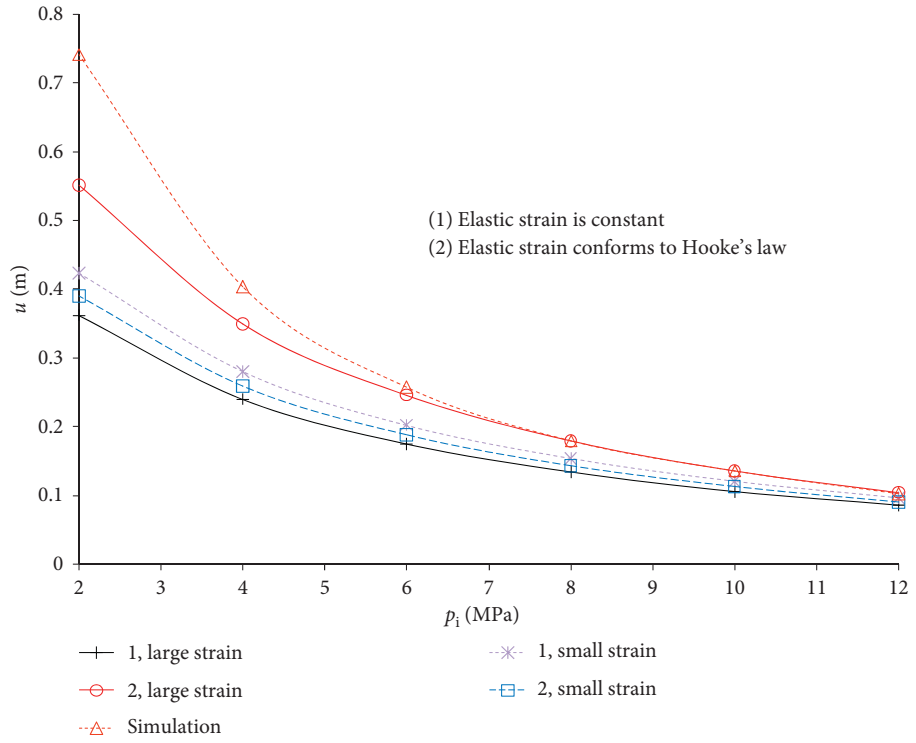

Figure 9: Relationships between displacements at the cavity wall and operating pressure (different elastic strain definitions and different strain theories).

Table 6: Creep model parameters of salt rock.

Viscous shear modulus G_0	3.8462 GPa
Viscous shear modulus G_1	12 GPa
Viscosity coefficient μ_1	200 GPa·h
Viscosity coefficient μ_2	800 GPa·h

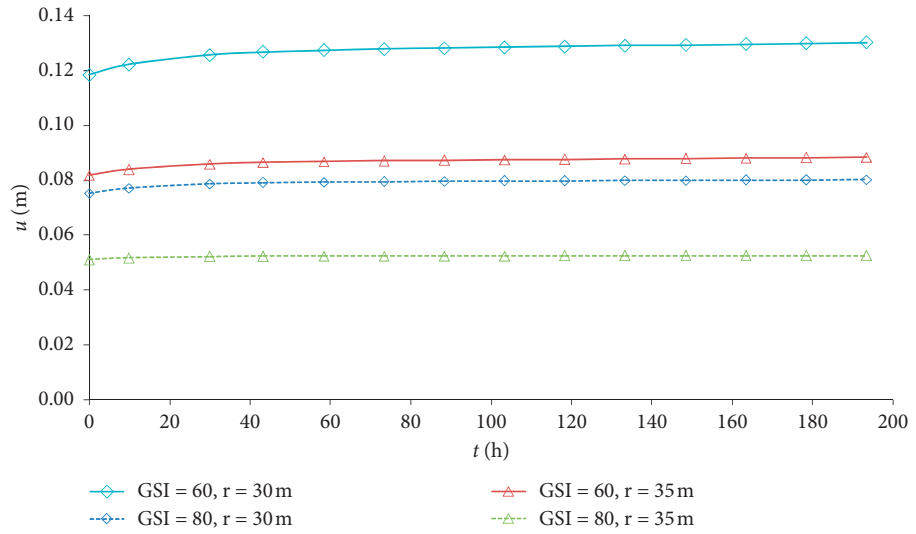

Figure 10: Displacement-time curves of surrounding rock at different positions.

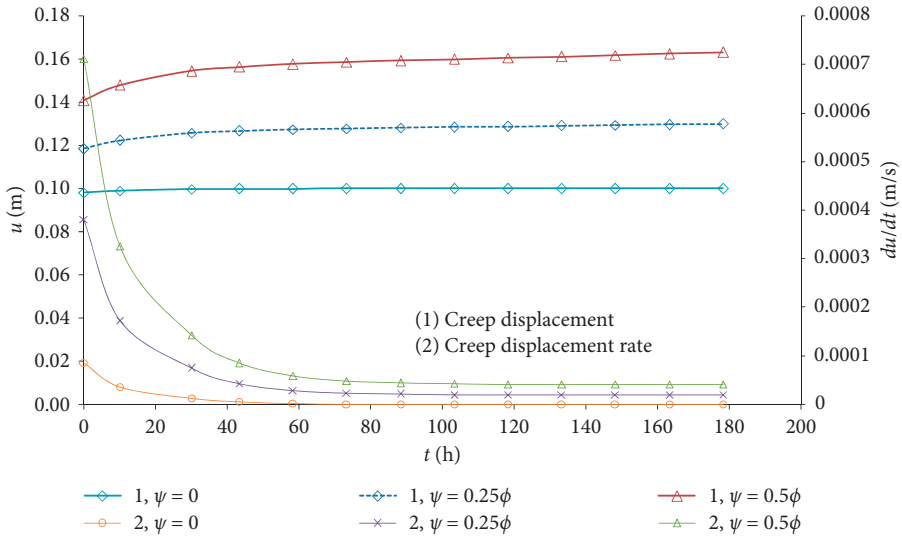

FIGURE 11: Creep displacement and displacement rate at the cavity wall (different dilation angels, $r = 30$ m).

and the effect increases with the enlarged dilation angle. The difference of displacements should be taken into account especially for poorly consolidated rock mass, such as permeable rock, rock formation with natural fractures, and water-soluble rock.

(3) The viscoelastic displacement analytical expression for the elastic and plastic zone has been obtained by adopting the same methodologies. The viscoelastic-plastic displacement variation of the surrounding rock is obtained by the viscoelastic-plastic analysis of the surrounding rock of the salt cavern with considering the creep strain. Analytical solutions are established based on the Nishihara creep model. The displacements decrease with the increasing H-B criterion parameter GSI in the viscoelastic or viscoplastic state, and the creep curve can enter the second creep stage faster. Both the visco-elastoplastic displacements and the creep displacement rate increase with the enlarged angle of dilation.

Data Availability

The data used to support the findings of this study are available from the corresponding author upon request.

Conflicts of Interest

The authors declare that they have no conflicts of interest.

Acknowledgments

This study was supported by the National Key R&D Program of China (grant no. 2017YFC1503102) and National Natural Science Foundation of China (grant no. 51504124).

References

[1] K.-H. Park and Y.-J. Kim, "Analytical solution for a circular opening in an elastic-brittle-plastic rock," *International Journal of Rock Mechanics and Mining Sciences*, vol. 43, no. 4, pp. 616–622, 2006.

[2] J.-S. Sun, W.-B. Lu, and Q.-H. Zhu, "Elasto-plastic analysis of circular tunnels in jointed rock masses satisfy the Hoek-Brown failure criterion," *Journal of China University of Mining and Technology*, vol. 17, no. 3, pp. 393–398, 2007.

[3] R. Jimenez, A. Serrano, and C. Olalla, "Linearization of the Hoek and Brown rock failure criterion for tunnelling in elasto-plastic rock masses," *International Journal of Rock Mechanics and Mining Sciences*, vol. 45, no. 7, pp. 1153–1163, 2008.

[4] M. Fraldi and F. Guarracino, "Limit analysis of collapse mechanisms in cavities and tunnels according to the Hoek-Brown failure criterion," *International Journal of Rock Mechanics and Mining Sciences*, vol. 46, no. 4, pp. 665–673, 2009.

[5] F. Rojat, V. Labiouse, and P. Mestat, "Improved analytical solutions for the response of underground excavations in rock masses satisfying the generalized Hoek-Brown failure criterion," *International Journal of Rock Mechanics and Mining Sciences*, vol. 79, pp. 193–204, 2015.

[6] H.-X. Wang, B. Zhang, and D. Fu, "Stability and airtightness of a deep anhydrite cavern group used as an underground storage space: a case study," *Computers and Geotechnics*, vol. 96, pp. 12–24, 2018.

[7] A. Lu, S. Wang, and X. Zhang, "Solution of the elasto-plastic interface of circular tunnels in Hoek-Brown media subjected to non-hydrostatic stress," *International Journal of Rock Mechanics and Mining Sciences*, vol. 106, pp. 124–132, 2018.

[8] B. Zhang, C. Laín, and M. C. Castañeda, "Mini-CAES as a reliable and novel approach to storing renewable energy in salt domes," *Energy*, vol. 144, pp. 482–489, 2018.

[9] X. C. Pous, "Elastoplastic theory analysis of axisymmetric roadway deformation," *Mechanics in Engineering*, vol. 16, no. 5, pp. 20–22, 1994.

[10] X. C. Liu and Y. M. Lin, "Theoretic analysis of elastoplastic deformation for the tunnel in soft rocks," *Rock and Soil Mechanics*, vol. 15, no. 2, pp. 27–36, 1994.

[11] Q. M. Luo, L. Li, and X. L. Yang, "The calculation of deformation of soft rock around tunnels," *Journal of Changsha Railway University*, vol. 21, no. 2, pp. 14–18, 2003.

[12] Y. Pan, G. M. Zhao, and X. R. Meng, "Elastro-plastic research of surrounding rock based on Hoek-Brown strength

criterion," *Journal of Engineering Geology*, vol. 19, no. 5, pp. 637–641, 2011.

[13] G. Y. Hou and X. S. Niu, "Perfect elastoplastic solution of axisymmetric cylindrical cavity based on levy-mises constitutive relation and Hoek-Brown failure criterion," *Chinese Journal of Rock Mechanics and Engineering*, vol. 29, no. 4, pp. 765–777, 2010.

[14] H. B. Cai, H. Cheng, and C. X. Rong, "Analysis on rock plastic zone displacement of deep buried underground chamber based on generalized Hoek-Brown criterion," *Journal of Mining and Safety Engineering*, vol. 32, no. 5, pp. 778–785, 2015.

[15] C. G. Zhang, W. Fan, and J. H. Zhao, "New solutions of rock plastic displacement and ground response curve for a deep circular tunnel and parametric analysis," *Rock and Soil Mechanics*, vol. 37, no. 1, pp. 12–24+32, 2016.

[16] J. F. Liu, Y. Bian, D. W. Zheng et al., "Discussion on strength analysis of salt rock under triaxial compressive stress," *Rock and Soil Mechanics*, vol. 35, no. 4, pp. 919–925, 2014.

[17] P. C. Wang and X. R. Zhu, "Analysis of cavity expansion in soil with shear dilation and strain softening considering large deformation," *Journal of Zhejiang University (Engineering Science)*, vol. 38, no. 7, pp. 116–121, 2004.

[18] S. B. Hu and X. R. Zhu, "Solution to spherical expansion of cavity in tri-linear strain-softening soil," *Bulletin of Science and Technology*, vol. 41, no. 6, pp. 848–852, 2007.

[19] G. S. Yao, J. P. Li, and S. C. Gu, "Analytic solution to deformation of soft rock tunnel considering dilatancy and plastic softening of rock mass," *Rock and Soil Mechanics*, vol. 30, no. 2, pp. 463–467, 2009.

[20] J. F. Zou, H. Luo, J. G. Peng et al., "Large-deformation analysis for cavity expansion in strain-softening soil," *China Journal of Highway and Transport*, vol. 22, no. 4, pp. 20–27, 2009.

[21] L. H. Zhang and H. J. Xiong, "Analytical solution for displacements of elasto viscoplastic ground around tunnel," *Chinese Jounal of Geotechnical Engineering*, vol. 19, no. 4, pp. 66–72, 1997.

[22] J. Sun, "Rock rheological mechanics and its advance in engineering applications," *Chinese Journal of Rock Mechanics and Engineering*, vol. 26, no. 6, pp. 1081–1106, 2007.

[23] L. Yuan, Z. N. Gao, and X. R. Meng, "Viscoelastic-plastic analysis of deep soft rock roadway based on drucker-prager criteria," *Mineral Engineering Research*, vol. 28, no. 1, pp. 11–16, 2013.

[24] G. Y. Hou, J. J. Li, B. Qiu et al., "Solving equation of rheological deformation in axisymmetric round well under dead load," *Rock and Soil Mechanics*, vol. 32, no. 2, pp. 341–346, 2011.

[25] S. Wen, Y. H. Liu, S. Q. Yang et al., "Rheological deformation of surrounding rock of circular tunnel based on the Hoek-Brown criterion," *Modern Tunnelling Technology*, vol. 30, no. 2, pp. 63–67, 2016.

[26] R. L. Cao, Q. W. Duan, Y. F. Zhao et al., "Hoek-Brown strength criterion and nishihara model-based visco-elasto-plastic solutions for circular tunnel," *Water Resources and Hydropower Engineering*, vol. 48, no. 4, pp. 64–71, 2017.

[27] E. Hoek and E. T. Brown, "The Hoek-Brown failure criterion and GSI–2018 edition," *Journal of Rock Mechanics and Geotechnical Engineering*, pp. 1–19, 2018.

[28] Q. Jiang, Y. Qi, and Z. Wang, "An extended Nishihara model for the description of three stages of sandstone creep," *Geophysical Journal International*, vol. 193, no. 2, pp. 841–854, 2013.

[29] C. Carranza-Torres and C. Fairhurst, "The elasto-plastic response of underground excavations in rock masses that satisfy the Hoek-Brown failure criterion," *International Journal of Rock Mechanics and Mining Sciences*, vol. 36, no. 6, pp. 777–809, 1999.